Journal of Food Engineering 306 (2021) 110642

Contents lists available at ScienceDirect

Journal of Food Engineering

journal homepage: http://www.elsevier.com/locate/jfoodeng

Rheological characterization of coconut cream emulsion using steady-state shear and time-dependent modeling

Avan Maghazechi [a], Abdorreza Mohammad Nafchi [a,b], Thuan-Chew Tan [a], Eng-Keng Seow [c], Azhar Mat Easa [a,*]

[a] Food Technology Division, School of Industrial Technology, Universiti Sains Malaysia, 11800, Penang, Malaysia
[b] Food Science and Technology Department, Damghan Branch, Islamic Azad University, Damghan, Iran
[c] Department of Food Science and Technology, Faculty of Applied Sciences, Universiti Teknologi MARA, 40450, Shah Alam, Selangor, Malaysia

ARTICLE INFO

Keywords:
Coconut-cream emulsion
Models
Rheological properties
Thixotropy
Time dependent

ABSTRACT

The rheological properties of raw coconut-cream emulsion (RCCE) were evaluated under various shear rates (0–500 s^{-1}) and temperatures (10 °C–50 °C) through steady-state shear and time-dependent modeling. Thixotropic behavior of the samples was observed at all temperatures tested, and it decreased with increased temperature. The Power law model was found to better fit the obtained data. The effects of temperature on regression parameters, namely, the Arrhenius and Turian relations were explored by approaches. The modeling parameters were assessed under the combined impacts of shearing and temperature, resulting in two generalized state equations governing the RCCE steady-state flow behavior. The extent and rate of thixotropy were measured with the Weltmann model, and the structural kinetics model was found to best describe the time-dependent behavior of RCCE. In conclusion, the structural breakdown was found in stress-decay tests at a high shear rate of 250 s^{-1} and a relatively high temperature of 50 °C.

1. Introduction

Coconut cream is a biologically complex multicomponent fluid extracted from mature coconut (*Cocos nucifera*). It primarily comprises carbohydrate, minerals, fats, and proteins. The fat percentage can be regulated according to the local requirement of around 15%–40% (Narataruksa et al., 2010). Coconut milk, a white oil-in-water emulsion, is physically unstable and tends to undergo phase separation. The separation of coconut milk into a cream-and-serum matrix commonly occurs within 5–10 h of manufacture (Jiang et al., 2016; Tangsuphoom and Coupland, 2009). Based on CODEX STAN240-2003, coconut milk is defined as a diluted emulsion originally derived from matured coconut kernel, whereas coconut cream is an undiluted emulsion extracted from the same mature kernel of the coconut.

Coconut products, including coconut milk, coconut water, and coconut cream, are perishable products because of their high fat and water content. Thus, coconut products are often thermally treated for pasteurization to extend their shelf life. Apart from pasteurization, ultra-high temperature treatment is used to generate a shelf-stable product, but only after long manufacturing processes. They start with peeling, grinding, and extraction, followed by sterilization or pasteurization through strong thermal treatment to inactivate heat-resistant enzymes and microorganisms. Ultimately, coconut milk or cream is pumped into a container. These all-mechanical processes involve the deformation and flow of material, referred to as rheological properties. Understanding the rheological characteristics of food aids quality control, plant conditions, structure, and equipment configuration (e.g., mixers, pump pipe, extruders, and heat exchangers) (Steffe, 1996). Rheological behavior also provides information regarding the physical properties of liquid foods to help elucidate the mechanisms underlying heat transfer and momentum (Kaur et al., 2002).

Fat content and temperature influence the apparent viscosity of coconut milk, as found in a previous study (Simuang et al., 2004). These factors reportedly play important roles in altering the rheological properties of coconut milk from processing to shelf storage. The heat-treatment effect on the flow properties of coconut milk has been previously studied, and coconut milk has been found to exhibit pseudoplastic behavior (Peamprasart and Chiewchan, 2006; Simuang et al., 2004; Tangsuphoom and Coupland, 2005). However, limited data regarding the applicability of time-dependent flow models in coconut

* Corresponding author.
E-mail address: azhar@usm.my (A.M. Easa).

https://doi.org/10.1016/j.jfoodeng.2021.110642
Received 4 November 2020; Received in revised form 29 March 2021; Accepted 12 April 2021
Available online 17 April 2021

cream are available. The impact of temperature on rheological properties requires documentation (Rao, 2013). Food dispersions need to be identified over time-dependent flow behaviors to determine the association between flow and structure and the relationship with other physical parameters (Roopa and Bhattacharya, 2009).

To the best of our knowledge, no research on the rheological properties of coconut cream at various temperatures, particularly detailed ones focusing on time-dependent rheological characterization, has been conducted. One of the most important factors required in designing a technological process in the food industry is a clear picture of rheological behavior. As a result, the primary objective of this study would be to categorize the flow behavior of RCCE, with an emphasis on their time-dependent properties as a function of shearing condition and temperature. Then, establishing generalized state equations governing flow behavior under the combined influences of temperature and shearing using predictive mathematical models.

2. Materials and methods

2.1. Sampling and proximate analysis

Mature coconuts (11–13 months old) were obtained from local markets in Penang, Malaysia, and nine nuts were randomly selected. They were shelled using a conventional coconut cutter before being peeled. After washing the fresh coconut meat, it was extracted and divided into the coconut cream and residues fibers (with no water added) using hydraulic pressure, followed by filtering through a cheesecloth to remove fibers. The prepared RCCE samples were refrigerated at 4 °C before analyses. Proximate composition (61.35% ± 0.15% moisture, 28.35% ± 0.08% fat, 3.21% ± 0.02% crude protein (N*5.30), 0.95% ± 0.01% ash, and 38.58% ± 0.04% total solids; pH 5.6 ± 0.3) was determined according to a previous study (AOAC, 2016).

2.2. Rheological measurements and modeling

Rheological analyses were conducted by Rheology Advantage Instrument Control AR (TA Instruments, New Castle, DE, USA). The experimental data obtained were analyzed with Rheology Advantage Data Analysis software V5.4.8 (TA Instruments, New Castle, DE, USA). A cone-plate sensor (40 mm diameter, 2° angle, and 0.051 mm gap) and a solvent trap were applied to minimize moisture loss during testing.

The conditions (shear rates and temperatures) in this work were selected from preliminary work conditions, starting from 10 °C to 95 °C. The conditions of the preliminary work were divided into two parts. The first part began from 10 °C to 50 °C as a cold and mild condition and was presented in the current research. The second part, involving high temperatures (70 °C–95 °C), will be used for further analysis. The division of the experimental conditions was based on the rheological behavior of the RCCE which shows two different rheological behavior during these regions, according to the instability of coconut emulsion.

2.2.1. Steady-state flow measurements with controlled shear rates (CSRs)

RCCE rheological behavior was examined at various temperatures (10, 20, 30, and 50 °C) by subjecting it to three stepwise continuous ramps (shear-rate ramps) as follows: (1) increasing the shear rate within the range of 0–500 s^{-1} for 5 min, (2) holding for 1 min at 500 s^{-1}, and (3) decreasing the shear rate within the range of 500–0 s^{-1} for another 5 min. The experimental results were fitted to the time-independent mathematical models of Ostwald–de Waele (known as the Power law) (Zarzycki et al., 2019) and Herschel–Bulkley (Herschel and Bulkley, 1926), as shown in Eqs. (1) and (2), respectively.

$$\tau = \mathrm{K}\,(\dot{\gamma})^{n} \quad \text{Equation (1)}$$

$$\tau = \tau_o + \mathrm{K}\,(\dot{\gamma})^{n} \quad \text{Equation (2)}$$

where τ is the shear stress (Pa), K is the consistency coefficient in ($Pa{\cdot}s^{n}$; a measure of apparent viscosity), $\dot{\gamma}$ is the shear rate (s^{-1}), n is the flow-behavior index (dimensionless), and τ_o is the yield shear stress (Pa).

Flow curves with CSR involved hysteresis cycles. Each cycle area (measured in $Pa{\cdot}s^{-1}$), calculated with TA Rheology Advantage (data-analysis application software), was simply the area of forward data points subtracted with the area of backward data points. The samples' apparent viscosities were evaluated using the Power law parameters (K and *n)* and then evaluated at specific shear rates (50, 100, 250, and 250 s^{-1}). The obtained set of apparent viscosity (η_a) values was used to calculate the effect of temperature at a specified shear rate by using an Arrhenius-type relation (Kobus et al., 2019), as shown in Eq. (3). To determine the Arrhenius-type relation parameters (η_0 and E_a), the equation was changed to a linear form by using natural logarithms, as shown in Eq. (4).

$$\eta_a = \eta_0 \exp(E_a / RT) \quad \text{Equation (3)}$$

$$\ln(\eta_a) = \ln(\eta_0) + \frac{E_a}{R} \times \frac{1}{T} \quad \text{Equation (4)}$$

where η_a is the apparent viscosity at a specific shear rate (mPa·s), η_0 is a pre-exponential factor at a specific temperature (mPa·s), E_a is the activation energy ($J{\cdot}mol^{-1}$), R is the universal gas constant ($J{\cdot}mol^{-1}{\cdot}K^{-1}$), and T is the temperature in Kelvin.

The influence of temperature on Power law parameters was evaluated with Turian relations, as shown in Eqs. (5) and (6) (Ramaswamy and Basak, 1991), in which α_1, β_1, α_2, and β_2 are linear coefficients.

$$in\,(K) = \alpha_1 - \beta_1\,(T) \quad \text{Equation (5)}$$

$$n = \alpha_2 + \beta_2\,(T) \quad \text{Equation (6)}$$

2.2.2. Stress-decay measurements at a constant shear rate (time dependency)

The samples were sheared at constant shear rates (5, 25, 50, 100, and 250 s^{-1}) and various temperatures (20, 30, and 50 °C). Shear stress and viscosity were calculated as a function of shear time until the equilibrium state was reached. Preliminary studies revealed that 10 min could sufficiently test RCCE samples and ensure that their rheological behavior no longer depended on shear time. The curves of shear–stress decay curves were examined using Weltmann model (Weltmann, 1943). In contrast, those of apparent-viscosity decay were explored with the second-order structural kinetics model (SKM) (Cao et al., 2019), as shown in Eqs. (7) and (8), respectively.

$$\tau = A - B\ln(t / t_m),\ t \geq t_m \quad \text{Equation (7)}$$

$$\left[\frac{(\eta - \eta_\infty)}{(\eta_0 - \eta_\infty)}\right]^{1-m} = (m-1)\,\kappa t + 1 \quad \text{Equation (8)}$$

where A and B are Weltmann parameters that represent the initial shear stress (Pa) and time coefficient of thixotropic breakdown (Pa), respectively; t is the shear time (s); t_m is the time at which the maximum shear stress ($t_m = 5$ s) is measured (s); η_0 is the initial viscosity (Pa·s); η_∞ is the equilibrium (steady-state) viscosity (Pa·s); κ is the decay (breakdown) rate constant (s^{-1}); and m is the reaction order decay were explored with the SKM approach assumes that the transition in time-dependent flow properties is consistent with the shear-induced breakdown of the internal fluid-structure from a structured state to a nonstructured one (Basim Abu-Jdayil, 2003; Dolores Alvarez and Canet, 2013; Tárrega et al., 2004).

2.3. Statistical analysis

The rheological measurements were curve fitted with the aforementioned mathematical models (Eqs. (1)–(8)) and statistically

analyzed using various indicators, primarily the coefficient of determination (R^2), Pearson's r, and the root–mean–square error. To investigate the reproducibility of results, three replicates were performed for all experiments, and the reproducibility was at ±5% on average. OriginPro 9.0 (OriginLab Corp., USA) was used to conduct statistical analyses.

3. Results and discussion

3.1. Flow behavior and thixotropy

The variations in shear stress as a function of shear rate applied to the RCCE samples at different temperatures (10 °C–50 °C) were determined, and results are plotted in Fig. 1(a). This procedure, a CSR test, clearly showed a logarithmic rise (in the forward-flow direction) in shear stress with steadily increased shear rate (about 100 s^{-1} per min). The plotted flow curves were nonlinear and followed non-Newtonian shear behavior, demonstrating the shear thinning of RCCE emulsion. Muda (2002) reported that low-concentration coconut milk has linear Newtonian behavior; conversely, at higher concentrations, it departs from linearity and follows the Power-law model, depicting shear-thinning (thixotropy) behavior. The hysteresis cycles are shown in Fig. 1(a) depict the thixotropic behavior of RCCE samples. This thixotropicity was associated with the breakdown of the fluid structure under continuous shearing deformation. The hysteresis area enclosed between the forward and backward flow curves represented the amount of energy required for a structural breakdown that was unrecovered during the experiment (Roopa and Bhattacharya, 2009). Table 1 shows the largest hysteresis area (699 Pa s^{-1}) at 10 °C and the smallest area (88.4 Pa s^{-1}) at 50 °C. The thixotropicity in RCCE may have contributed to the instability of this emulsion. Coconut cream emulsion is naturally stabilized by its proteins, such as globulins, albumins, and phospholipids. However, the insufficient quantity and quality of these proteins caused poor emulsifying properties, which lead to the instability of the coconut cream emulsion (Tangsuphoom and Coupland, 2008). Their emulsifying properties are influenced by their structure, which is affected by environmental factors, such as temperature (Tangsuphoom and Coupland, 2009). As a result, the shearing of RCCE caused mechanical instabilities (coalescence), and this irreversible change induced the time-dependent behavior (Schoff and Kamarchik, 2005).

The thixotropic behavior was more pronounced at low temperature (10 °C) and was significantly reduced with increased temperature until 50 °C. As pointed out by (Ariyaprakai and Tananuwong, 2015), the fat of coconut milk emulsions exists in the form of crystals at temperatures lower than 24 °C. This phenomenon affects the rheological behavior of

Table 1
Power law parameters evaluated at different temperatures, with hysteresis areas.

°C	*Forward Flow*			*Backward Flow*			Hysteresis area (Pa. s^{-1})
	K (mPa. s^n)	*N*	R^2	K (mPa. s^n)	*n*	R^2	
10	197.86 ± 3.589	0.619 ± 0.031	0.998	33.63 ± 0.368	0.889 ± 0.001	0.999	699 ± 15.301
20	69.22 ± 2.545	0.734 ± 0.018	0.997	36.27 ± 1.137	0.840 ± 0.055	0.998	280 ± 12.142
30	46.53 ± 1.328	0.780 ± 0.011	0.999	20.45 ± 0.205	0.905 ± 0.001	0.999	253 ± 9.035
50	12.69 ± 0.849	0.903 ± 0.009	0.999	13.72 ± 0.147	0.822 ± 0.022	0.999	88.4 ± 23.265

Data are expressed as arithmetic mean (n = 3) ± standard deviation (SD).

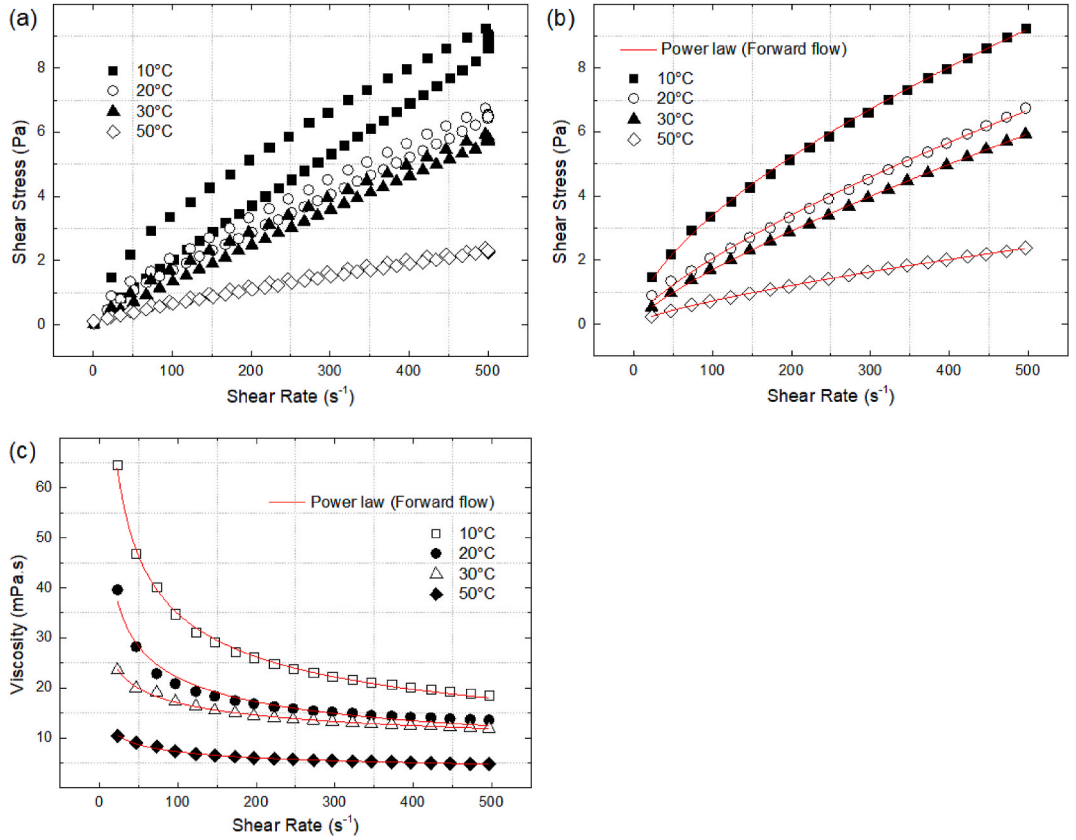

Fig. 1. Flow curves of RCCE samples at different temperatures, (a) Hysteresis-cycles, (b) Flow behavior modeling using the Power law, in terms of shear stress, and (c) modeling in terms of apparent viscosity (η_a).

RCCE and leads to emulsion instability under shearing, which ultimately results in droplet aggregation through partial coalescence (McClements, 2015). Consequently, it increased the thixotropicity of RCCE.

Two rheological models, namely, Power law and Herschel–Bulkley, were applied to fit the RCCE experimental data. Tables 1 and 2 present the model-fitting parameters determined for forward and backward flows. The fitting parameters obtained from the Power law had a clear trend, i.e., the flow index (n) increased with increased temperature; conversely, the consistency coefficient (K) decreased with increased temperature. This finding was in accordance with the vast majority of literature dealing with other food emulsions (Basim Abu-Jdayil, Al-Malah and Asoud, 2002; Abu-Jdayil, Shaker and Jumah, 2000; Deswal et al., 2014). At 10 °C, the highest yield-stress value of the Herschel–Bulkley model was obtained, which can be explained by greater interarticular forces at low temperatures than at higher ones (Alonso et al., 1995; Dolores Alvarez and Canet, 2013). The obtained yield-stress fits contributed considerably less with increased temperature until 50 °C. Although both mathematical models were well fitted with high correlation values ($R^2 \geq 0.999$), the model-fitting parameters had trends that favored the Power-law model more than their counterparts in the Herschel–Bulkley model. Moreover, the SD for the Herschel-Bulkley model's consistency coefficient was higher than that in the Power-law model. These could account for the fact that the Power-law model may better describe the flow behavior of these products. This result supported a previous finding (Muda, 2002) that coconut milk (25%–50% TS) behaves more like a Power-law fluid.

Additionally, Fig. 1(b) and (c) show the forward-flow experimental data fit by using the Power-law model in terms of shear stress and apparent viscosity, respectively. At higher temperatures, the flow curves became lower and tended to behave more like a Newtonian liquid because of the increasingly combined effect of shearing and temperature. With increased shear rate, the flow encountered less resistance, so the viscosity levels decreased. Viscosity then decreased under the shear rate of 0–50 s^{-1} such that it reflected low flow resistance. The tested samples exhibited a very clear non-Newtonian (shear-thinning) behavior within the range of 50–250 s^{-1}, although the trend approached Newtonian behavior at shear rates of 250–500 s^{-1}, as evidenced by the viscosity reaching a plateau. Given that coconut cream is a type of suspension system, its viscosity depended on shear rate. RCCE at a low shear rate had high viscosity. With increased shear rate, the hydrodynamic forces became more significant. The emulsion particles eventually became oriented with the flow path, so the viscosity tended toward a constantly low value (Ariffin et al., 2016). The power-law model was found to be suitable for describing the flow of RCCE after eliminating the time dependency.

3.2. Combined effect of temperature and shearing on flow parameters

Fig. 2 is a plot of the effect of temperature on apparent viscosity by using Eq. (4), with high correlation figures (Pearson's r of 0.998 and 0.994 for 250 s^{-1} and 500 s^{-1} rate, respectively). The regression parameters at selected shear rates are shown in Table 3. The calculated activation energies presented a clear trend in the forward flow, i.e., activation energies decreased with increased shear rate (Simuang et al., 2004; Steffe, 1996; Telis-Romero et al., 1999). Meanwhile, in the backward flow, the calculated E_a values were relatively independent of the shear-rate effect. Moreover, the (η_o) viscosity values tended to decrease with increased shear rate (in forward flow) and reversibly in the backward flow. The effect of temperature on K and n set of values was plotted using Eqs. (5) and (6), as presented in Fig. 3(a) and (b). The value of K, which is considered as a measure of viscosity, decreased with increased temperature. In contrast, n values had an inverse trend because they increased with increased temperature, as described in the previous section. High correlation figures were obtained in modeling K and n with respect to temperature (Pearson's $R \geq 0.98$). Overall, based on the obtained linear relations of K and n tested within the range of 10 °C–50 °C, two generalized state equations were established for RCCE under the combined effect of shearing and temperature (in forward and backward flows), as shown in Eqs. (9) and (10) (derived from the logarithmic form of the Power law and using Eqs. (5) and (6) to derive the relationship of K and n with temperature).

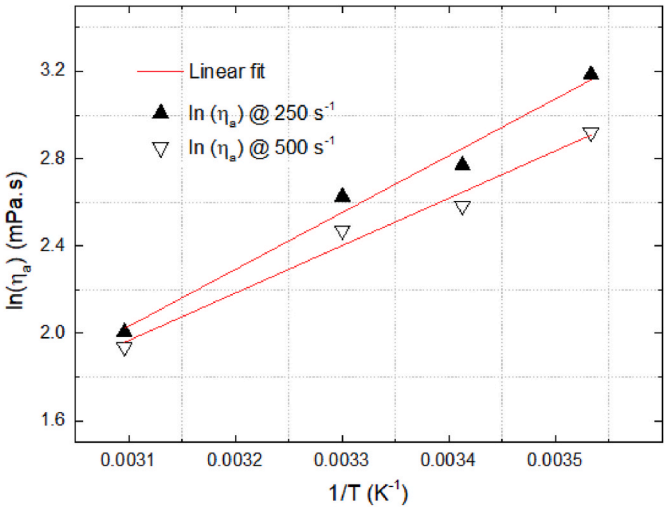

Fig. 2. Effect of temperature on apparent viscosity (Forward flow) at shear rates of 250 s^{-1} ▲ and 500 s^{-1} ▽, over (10–50 °C) temperature range, using Eq. (4).

$$\tau_{(forward)} = \exp(5.78492 - 0.06576(T)) \times \dot{\gamma}^{0.57263+0.00678(T).} R^2 \geq 0.975$$

Equation (9)

$$\tau_{(backward)} = \exp(3.87671 - 0.0251(T)) \times \dot{\gamma}^{0.89857+0.00126\ (T).} R^2 \geq 0.955$$

Equation (10)

where τ is the shear stress (mPa), $\dot{\gamma}$ is the shear rate (s^{-1}), and T is the temperature (°C).

3.3. Time-dependent analysis

Results of thixotropic-behavior analysis (based on RCCE flow-hysteresis cycles and their respective calculated areas) revealed that rheological properties were time-dependent. Using the Weltmann model, stress-decay tests were conducted to measure the rate and extent

Table 2
Herschel-Bulkley model parameters at different temperatures.

°C	*Forward flow*				*Backward flow*			
	τ_o (Pa)	K (mPa.s^n)	*n*	R^2	τ_o (Pa)	K (mPa.s^n)	*N*	R^2
10	0.386 ± 0.054	150.5 ± 4.103	0.678 ± 0.015	0.999	0.058 ± 0.008	30.84 ± 0.663	0.903 ± 0.023	0.999
20	0.462 ± 0.011	31.88 ± 3.218	0.849 ± 0.024	0.999	0.131 ± 0.010	27.56 ± 0.413	0.877 ± 0.035	0.998
30	0.078 ± 0.005	40.89 ± 2.012	0.802 ± 0.043	0.999	−0.019 ± 0.002	21.38 ± 0.546	0.898 ± 0.002	0.999
50	0.016 ± 0.003	22.66 ± 0.913	0.748 ± 0.004	0.999	−0.003 ± 0.003	13.91 ± 0.272	0.820 ± 0.024	0.999

Data are expressed as arithmetic mean (n = 3) ± SD.

Table 3
Arrhenius-type relation parameters evaluated at selective shear rates.

$\dot{\gamma}$ (s^{-1})	*Forward flow*				*Backward flow*			
	E_a (kJ/mol)	η_o (mPa.s)	Pearson's r	RMSE	E_a (kJ/mol)	η_o (mPa.s)	Pearson's R	RMSE
50	30.000	1.23×10^{-4}	0.995	0.103	22.754	1.54×10^{-3}	0.977	0.135
100	26.399	4.42×10^{-4}	0.997	0.091	23.404	1.08×10^{-3}	0.976	0.142
250	21.637	2.39×10^{-3}	0.998	0.077	24.263	6.76×10^{-4}	0.972	0.159
500	18.036	8.59×10^{-3}	0.994	0.068	24.913	4.74×10^{-4}	0.968	0.175

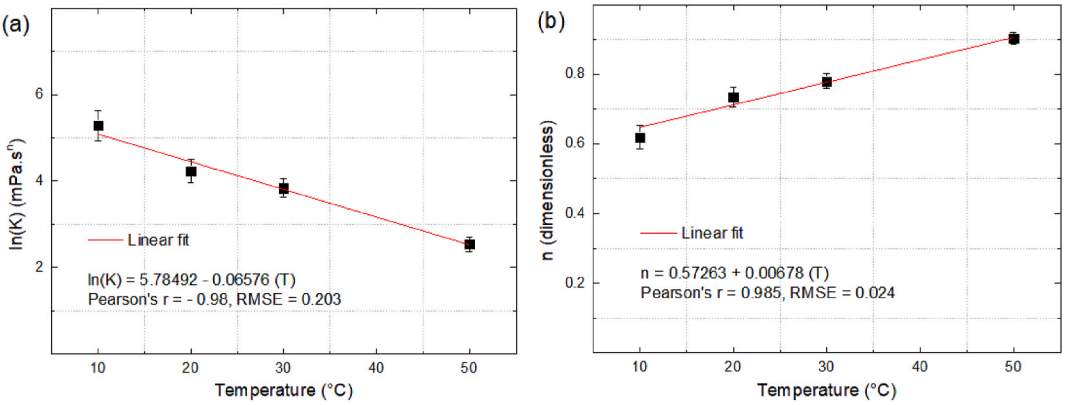

Fig. 3. Effect of temperature on Power law parameters (Forward flow), using Turian relations, (Eqs. (5) and (6)). **(a)** Consistency coefficient – K, and **(b)** Flow behavior index – *n*.

of RCCE thixotropy. This model was based on the logarithmic decay in shear stress with shear time (Eq. (7)). Fig. 4(a) and (c) present Weltmann model fits at (50 °C) and at constant shearing (250 s^{-1}), respectively. No significant structural breakdown occurred at low shear rates (5, 25, 50, and 100 s^{-1}) (as manifested by the flatness of decay curves). Shearing at a rate of 250 s^{-1} and at ≥30 °C departed from such flatness. This result could be substantiated by a previous report (Junqueira et al., 2018) of the unaltered inner surface upon applying low shear stress. The regression parameters A and B are presented in Table 4. Their values showed a clear trend owing to the combined effect of temperature and

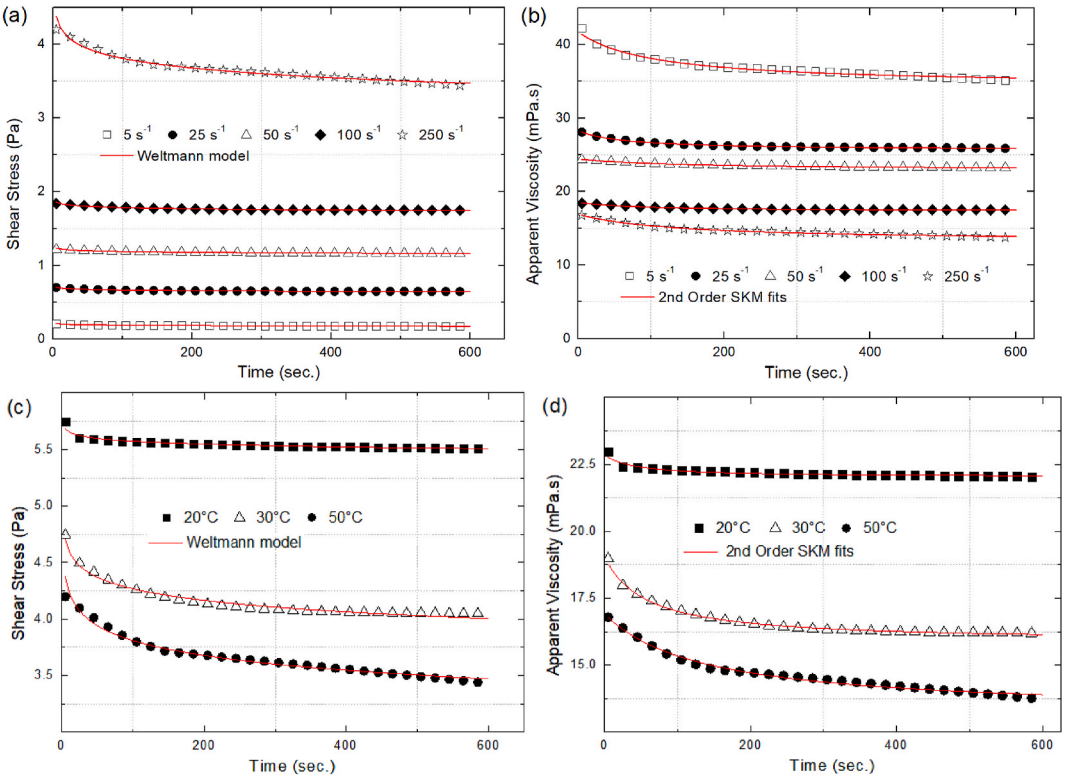

Fig. 4. Stress decay experiments using Weltmann model fits, and Second-order SKM fits. (a) and (b) using different shear rates (5, 25, 50, 100, and 250 s^{-1}) at 50 °C, while (c) and (d) were done at 250 s^{-1}, over selected temperatures (20, 30, and 50 °C).

Table 4
Time-dependent flow fitting parameters at selective temperatures of (20–50 °C).

°C	$\dot{\gamma}$ (s^{-1})	*Weltmann model*			*Second-order SKM*		
		A (× 10^{-2} Pa)	B (× 10^{-2} Pa)	R^2	κ (× 10^{-2} s^{-1})	η_o/η_∞	R^2
20	5	49.62 ±	1.39 ±	0.997	6.49 ±	1.402 ±	0.999
	25	0.01	0.01	0.998	0.006	0.03	0.999
	50	98.01 ±	2.53 ±	0.997	8.43 ±	1.225 ±	0.999
	100	0.01	0.07	0.998	0.005	0.04	0.998
	250	159.92 ±	3.43 ±	0.996	10.45 ±	1.158 ±	0.999
		0.04	0.03		0.004	0.01	
		278.17 ±	3.53 ±		11.94 ±	1.095 ±	
		0.30	0.06		0.002	0.02	
		574.15 ±	3.65 ±		15.06 ±	1.020 ±	
		0.08	0.01		0.003	0.02	
30	5	32.05 ±	0.97 ±	0.997	7.29 ±	1.282 ±	0.999
	25	0.02	0.01	0.998	0.003	0.07	0.999
	50	88.75 ±	2.31 ±	0.997	9.67 ±	1.165 ±	0.999
	100	0.01	0.02	0.999	0.006	0.02	0.997
	250	142.11 ±	3.11 ±	0.997	11.76 ±	1.112 ±	0.999
		0.06	0.05		0.009	0.03	
		251.53 ±	7.40 ±		13.84 ±	1.064 ±	
		0.05	0.02		0.002	0.08	
		494.51 ±	14.71 ±		17.50 ±	1.010 ±	
		0.21	0.03		0.002	0.03	
50	5	22.46 ±	0.75 ±	0.999	8.42 ±	1.213 ±	0.998
	25	0.06	0.03	0.997	0.005	0.07	0.999
	50	72.43 ±	1.24 ±	0.997	12.55 ±	1.110 ±	0.999
	100	0.08	0.01	0.996	0.003	0.01	0.999
	250	125.95 ±	1.53 ±	0.999	15.34 ±	1.075 ±	0.999
		0.05	0.02		0.001	0.03	
		219.79 ±	9.41 ±		20.21 ±	1.039 ±	
		0.10	0.02		0.001	0.09	
		468.29 ±	18.95 ±		24.81 ±	1.001 ±	
		0.10	0.04		0.007	0.06	

Data are expressed as arithmetic mean (n = 3) ± SD.

shear rate. Weltmann A parameter represented the shear stress needed for the structure to start degrading (initial stress). In contrast, the Weltamnn B parameter indicated the amount of structure damaged during shearing (time coefficient of thixotropic breakdown) (Dolores Alvarez and Canet, 2013). Weltmann A values decreased with increased temperature, indicating a reduction in RCCE flow resistance. Moreover, the extent of thixotropy embodied by the magnitude of Weltamnn B (Basim Abu-Jdayil et al., 2002) tended to decrease with the increased temperature at lower shear rates (5, 25, and 50 s^{-1}), whereas it increased with increased temperature at higher rates (100 and 250 s^{-1}). The use of the Weltmann model to quantify thixotropy was found satisfactory for describing RCCE experimental data at constant shear rates ($R^2 \geq 0.996$).

Furthermore, SKM was used to explore the parameters of viscosity change with time (viscosity decay) at different shear rates with selected temperatures (20, 30, and 50 °C), and results are shown in Fig. 4(b) and (d). Viscosity rapidly decreased at the initial stages of shearing within the first 150 s, indicating a progressive breakdown of coconut cream structure by configuring the proteins and fat in the coconut-cream emulsion (Basim Abu-Jdayil, 2003). It then levelled off after 150 s toward 600 s. Table 4 details the SKM parameters determined to describe our experimental data. The κ parameter (s^{-1}) represents the rate of structural breakdown (degree of thixotropy), whereas the ratio of initial over steady-state viscosity (η_o/η_∞) is the amount of breakdown (the extent of thixotropy) (B. Abu-Jdayil, 2004). The values of (κ) and (η_o/η_∞) were significantly influenced by shear rate and temperature. Apparent viscosity considerably decreased with time, and the decay constant (κ) values considerably increased with increased shearing at all studied temperatures. The SKM approach for modeling thixotropic behavior in RCCE samples was able to describe the experimental data satisfactorily ($R^2 \geq 0.997$).

3.4. Influence of shear rate on stress-decay parameters

To further explore the modeling of RCCE stress decay experiments, the relations of modeling parameters with shear rate were investigated. The selected parameters were related to the best fits of the SKM and Weltmann models. The Power law was successfully used ($R^2 \geq 0.99$) to fit all parameters (Weltmann's A, Weltmann's B, decay-rate constant κ, and thixotropy extent ratio (η_o/η_∞)) versus shear rates (5, 25, 50, 100, and 250 s^{-1}), and results are shown in Fig. 5(a), (b), 6(a) and 6(b), respectively. Table 5 lists the obtained generalized state equations. The state-equations modeling the thixotropy behavior of RCCE were primarily derived from the emulsion instability and structural degradation under constant-shearing experiments. The parameters Weltmann A and B rapidly increased with increased shearing but decreased with increased temperature. The constant decay κ directly corresponded with the influences of shearing and temperature, whereas the thixotropy extent ratio (η_o/η_∞) was inversely related to both of these effects.

3.5. Effect of temperature on stress-decay parameters

The modeling works are incomplete without relating the decay parameters to temperature (Dolores Alvarez and Canet, 2013). Upon selecting Weltmann A parameters, the heat-treatment effect was examined using an Arrhenius-type modified relation (Eq. (4)). Each apparent viscosity (η_a) value was determined using the relation ($A/\dot{\gamma}$) followed by taking the natural logarithm of this relation and plotting it against the reciprocal of temperature ($1/T$). The obtained linear plots provided information on activation energies together with the steady-state viscosities (η_∞) from plot intercepts, as shown in Fig. 7. Table 6 summarizes these results, and the fitted trends were found to be acceptable ($R^2 \geq 0.90$). High η_∞ and low E_a values indicated that the maximum degree of orientation and the minimum attainable viscosity were achieved.

4. Conclusion

Rheological characterization of RCCE exhibited its thixotropic behavior at all studied temperatures (10–50 °C) within the shearing range of 0–500 s^{-1}. The thixotropicity considerably decreased with increased temperature, whereas molecular-structure breakdown became more apparent at lower temperatures that changed the rheological properties. CSR testing results were explained better by the Power-law model. The modeling parameters were evaluated under the combined effects of shearing and temperature, resulting in two generalized state equations.

To evaluate structural degradation in terms of rate and amount, a time-dependent analysis was performed using decay experiments at constant shearing. Modeling was satisfactorily conducted using the Weltmann model and SKM approach. Structural degradation was evident at high shearing (250 s^{-1}) and at ≥30 °C. In conclusion, the rheological characterization of RCCE under various temperatures and shearing conditions can be used to design a thermal process for RCCE production. These findings should be followed up with further work focusing on higher temperatures.

Credit author statement

Avan Maghazechi: Methodology, Validation, Formal analysis, Investigation, Resources, Data curation, Writing – original draft. Abdorreza Mohammad Nafchi: Methodology, Validation, Formal analysis, Investigation, Resources, Data curation, Writing – review & editing, Supervision. Thuan-Chew Tan: Validation, Resources, Writing – review & editing, Supervision, Project administration. Eng-Keng Seow: Validation, Formal analysis, Data curation, Writing – review & editing, Supervision. Azhar Mat Easa: Conceptualisation, Methodology, Validation, Writing – review & editing, Supervision, Project administration.

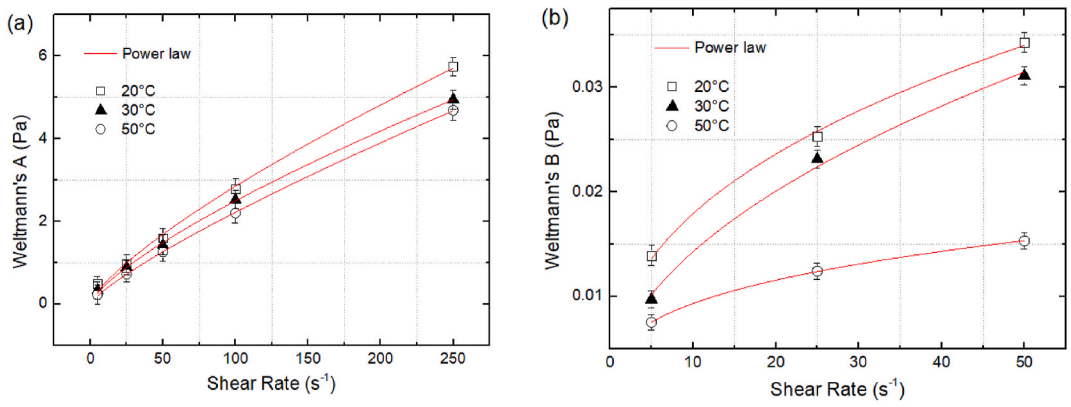

Fig. 5. Weltmann model parameters as a function of shear rate, (a) Weltmann's A, and (b) Weltmann's B.

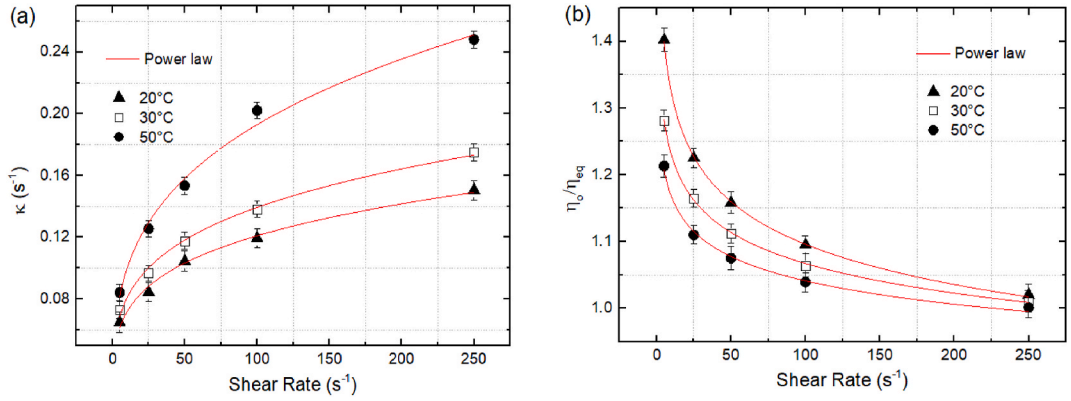

Fig. 6. Second-order structural kinetics model parameters as a function of shear rate (at 20, 30, and 50 °C), (a) Decay rate constant – κ, and (b) Thixotropy extent ratio (η_o/η_∞).

Table 5
Thixotropy state-equations for decay models parameters as a function of shear rate.

°C	Weltmann's A (mPa)	R^2	Weltmann's B (mPa)	R^2	Decay constant κ (s^{-1})	R^2	η_o/η_∞	R^2
20	$81.4\ \dot{\gamma}^{0.770}$	0.997	$7.17\ \dot{\gamma}^{0.398}$	0.997	$0.426\ \dot{\gamma}^{0.227}$	0.991	$1.597\ \dot{\gamma}^{-0.082}$	0.998
30	$78.6\ \dot{\gamma}^{0.750}$	0.999	$4.62\ \dot{\gamma}^{0.490}$	0.996	$0.469\ \dot{\gamma}^{0.237}$	0.993	$1.416\ \dot{\gamma}^{-0.062}$	0.999
50	$51.9\ \dot{\gamma}^{0.815}$	0.999	$4.57\ \dot{\gamma}^{0.309}$	0.999	$0.515\ \dot{\gamma}^{0.287}$	0.991	$1.309\ \dot{\gamma}^{-0.050}$	0.998

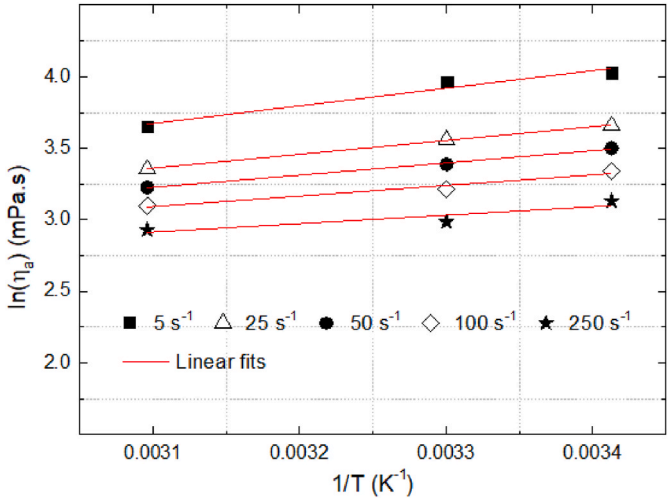

Fig. 7. Effect of temperature on apparent viscosity (derived from Weltmann's A parameter), at shear rates of (5, 25, 50, 100, and 250 s^{-1}), using Eq. (4).

Table 6
Activation energies and steady-state viscosities, derived from modified Arrhenius relation (Eq. (4)), based on the use of Weltmann's A parameter.

$\dot{\gamma}$ (s^{-1})	E_a ($kJ.mol^{-1}$)	η_∞ (mPa.s)	R^2	RMSE
5	10.214	0.873	0.96	0.054
25	8.030	1.444	0.99	0.007
50	7.089	1.792	0.99	0.012
100	6.148	2.225	0.96	0.032
250	4.904	2.962	0.90	0.059

Declaration of competing interest

The authors declare that they do not have any conflict of interest.

Acknowledgments

This study was funded by Fundamental Research Grant Scheme (FRGS) awarded by Ministry of Higher Education Malaysia (Grant No: 203/PTEKIND/6711812). We gratefully acknowledge and are indebted to the anonymous referees for comments and constructive suggestions provided for improving the manuscript.

Appendix A. Supplementary data

Supplementary data related to this article can be found at https://doi.org/10.1016/j.jfoodeng.2021.110642.

References

Abu-Jdayil, B., 2003. Modeling the time-dependent rheological behavior of semisolid foodstuffs. J. Food Eng. 57 (1), 97–102. https://doi.org/10.1016/S0260-8774(02)00277-7.

Abu-Jdayil, B., 2004. Flow properties of sweetened sesame paste (halawa tehineh). European food research and technology = Zeitschrift fur Lebensmittel-Untersuchung und -Forschung A 219 (3), 265–272. https://doi.org/10.1007/s00217-004-0959-5.

Abu-Jdayil, B., Al-Malah, K., Asoud, H., 2002. Rheological characterization of milled sesame (tehineh). Food Hydrocolloids 16 (1), 55–61. https://doi.org/10.1016/S0268-005X(01)00040-6.

Abu-Jdayil, B., Shaker, R.R., Jumah, R.Y., 2000. Rheological behavior of concentrated yogurt (Labneh). Int. J. Food Prop. 3 (2), 207–216. https://doi.org/10.1080/10942910009524628.

Alonso, M.L., Larrode, O., Zapico, J., 1995. Rheological behaviour OF infant foods. J. Texture Stud. 26 (2), 193–202. https://doi.org/10.1111/j.1745-4603.1995.tb00793.x.

Aoac, 2016. Official Methods of Analysis of AOAC International. AOAC International, Rockville, MD, ISBN 978-0-935584-87-5.

Ariffin, T.S.T., Yahya, E., Husin, H., 2016. The rheology of light crude oil and water-in-oil-emulsion. Procedia Engineering 148, 1149–1155. https://doi.org/10.1016/j.proeng.2016.06.614.

Ariyaprakai, S., Tananuwong, K., 2015. Freeze–thaw stability of edible oil-in-water emulsions stabilized by sucrose esters and Tweens. J. Food Eng. 152, 57–64. https://doi.org/10.1016/j.jfoodeng.2014.11.023.

Cao, V.D., Salas-Bringas, C., Barfod Schüller, R., Szczotok, A.M., Kjøniksen, A.-L., 2019. Time-dependent structural breakdown of microencapsulated phase change materials suspensions. J. Dispersion Sci. Technol. 40 (2), 179–185. https://doi.org/10.1080/01932691.2018.1462194.

Deswal, A., Deora, N.S., Mishra, H.N., 2014. Effect of concentration and temperature on the rheological properties of oat milk. Food Bioprocess Technol. 7 (8), 2451–2459. https://doi.org/10.1007/s11947-014-1332-8.

Dolores Alvarez, M., Canet, W., 2013. Time-independent and time-dependent rheological characterization of vegetable-based infant purees. J. Food Eng. 114 (4), 449–464. https://doi.org/10.1016/j.jfoodeng.2012.08.034.

Herschel, W.H., Bulkley, R., 1926. Konsistenzmessungen von Gummi-benzollösungen. Kolloid Z. 39 (4), 291–300. https://doi.org/10.1007/BF01432034.

Jiang, P., Xiang, D., Wang, X., 2016. Effect of different treatment on the properties of coconut milk emulsions. Food Sci. Technol. Res. 22 (1), 83–89. https://doi.org/10.3136/fstr.22.83.

Junqueira, L.A., Amaral, T.N., Leite Oliveira, N., Prado, M.E.T., de Resende, J.V., 2018. Rheological behavior and stability of emulsions obtained from Pereskia aculeata Miller via different drying methods. Int. J. Food Prop. 21 (1), 21–35. https://doi.org/10.1080/10942912.2018.1437177.

Kaur, S., Kaler, R.S.S., Aamarpali, 2002. Effect of starch on the rheology of molasses. J. Food Eng. 55 (4), 319–322. https://doi.org/10.1016/s0260-8774(02)00108-5.

Kobus, Z., Nadulski, R., Wilczyński, K., Starek, A., Zawiślak, K., Rydzak, L., Andrejko, D., 2019. Modeling of rheological properties of cloudy apple juice using master curve. CyTA - J. Food 17 (1), 648–655. https://doi.org/10.1080/19476337.2019.1630484.

McClements, D.J., 2015. Food Emulsions: Principles, Practice, and Techniques, 3rd ed.), third ed. CRC Press Taylor & Francis.

Muda, N., 2002. Rheological Behaviour of Coconut Milk: Effects of Concentration and Temperature. Universiti Putra Malaysia.

Narataruksa, P., Pichitvittayakarn, W., Heggs, P.J., Tia, S., 2010. Fouling behavior of coconut milk at pasteurization temperatures. Appl. Therm. Eng. 30 (11), 1387–1395. https://doi.org/10.1016/j.applthermaleng.2010.02.028.

Peamprasart, T., Chiewchan, N., 2006. Effect of fat content and preheat treatment on the apparent viscosity of coconut milk after homogenization. J. Food Eng. 77 (3), 653–658. https://doi.org/10.1016/j.jfoodeng.2005.07.024.

Ramaswamy, H., Basak, S., 1991. Rheology of stirred yogurts. J. Texture Stud. 22 (2), 231–241.

Rao, M.A., 2013. Flow and functional models for rheological properties of fluid foods. In: Food Engineering Series. Springer US, pp. 27–61.

Roopa, B.S., Bhattacharya, S., 2009. Characterization and modeling of time-independent and time-dependent flow behaviour of sodium alginate dispersions. Int. J. Food Sci. Technol. 44 (12), 2583–2589. https://doi.org/10.1111/j.1365-2621.2009.02088.x.

Schoff, C.K., Kamarchik Jr., P., 2005. Rheology and rheological measurements. In: Kirk-Othmer Encyclopedia of Chemical Technology. https://doi.org/10.1002/0471238961.1808051519030815.a01.pub2.

Simuang, J., Chiewchan, N., Tansakul, A., 2004. Effects of fat content and temperature on the apparent viscosity of coconut milk. J. Food Eng. 64 (2), 193–197. https://doi.org/10.1016/j.jfoodeng.2003.09.032.

Steffe, J.F., 1996. Rheological Methods in Food Process Engineering. Freeman Press.

Tangsuphoom, N., Coupland, J.N., 2005. Effect of heating and homogenization on the stability of coconut milk emulsions. J. Food Sci. 70 (8), e466–e470. https://doi.org/10.1111/j.1365-2621.2005.tb11516.x.

Tangsuphoom, N., Coupland, J.N., 2008. Effect of surface-active stabilizers on the microstructure and stability of coconut milk emulsions. Food Hydrocolloids 22 (7), 1233–1242. https://doi.org/10.1016/j.foodhyd.2007.08.002.

Tangsuphoom, N., Coupland, J.N., 2009. Effect of thermal treatments on the properties of coconut milk emulsions prepared with surface-active stabilizers. Food Hydrocolloids 23 (7), 1792–1800.

Tárrega, A., Durán, L., Costell, E., 2004. Flow behaviour of semi-solid dairy desserts. Effect of temperature. Int. Dairy J. 14 (4), 345–353. https://doi.org/10.1016/j.idairyj.2003.12.004.

Telis-Romero, J., Telis, V.R.N., Yamashita, F., 1999. Friction factors and rheological properties of orange juice. J. Food Eng. 40 (1), 101–106. https://doi.org/10.1016/S0260-8774(99)00045-X.

Weltmann, R.N., 1943. Breakdown of thixotropic structure as function of time. J. Appl. Phys. 14 (7), 343–350. https://doi.org/10.1063/1.1714996.

Zarzycki, P., Ciolkowska, A.E., Jablonska-Rys, E., Gustaw, W., 2019. Rheological properties of milk-based desserts with the addition of oat gum and kappa-carrageenan. J. Food Sci. Technol. 56 (11), 5107–5115. https://doi.org/10.1007/s13197-019-03983-4.